



DOI: 10.34910/MCE.102.8

Numerical investigation of truss-shaped braces in eccentrically braced steel frames

M. Haji, F. Azarhomayun, A.R. Ghiami Azad*

University of Tehran, Tehran, Iran

*E-mail: rghiami@ut.ac.ir

Keywords: finite element method, cyclic loads, stainless steel, buckling, hysteresis, eccentric brace

Abstract. Eccentrically braced frames are one of the most popular systems in buildings because they provide both high stiffness and ductility to the structure. Other systems such as moment frames and concentrically braced frames do not usually provide desirable stiffness and ductility, respectively. Steel shear walls are also popular systems in steel buildings; however, they can be expensive due to the large amount of steel used in these systems. Therefore, it is of interest to investigate new types of eccentrically braced frames. In this paper a truss-shaped brace is proposed and its behavior under cyclic loading in an eccentrically braced frame is numerically investigated using finite element software. Different cross-sections are implemented in the truss-shaped brace and the effect of the cross-section on the behavior of the frame is studied and compared to the reference specimen with conventional configuration. The results of this study show that hollow square cross-section with 100 mm width and 4 mm thickness had the best performance in terms of strength, absorbed energy and pinching compared to other specimens.

1. Introduction

Among seismic lateral load-bearing systems, moment frames, special moment frames in specific, can be considered as seismic load-bearing systems that have high ductility and low stiffness. On the other hand, concentrically braced frames despite having high stiffness, do not have high ductility. In other words, the displacement criterion usually controls the design of special moment frames, whereas in concentrically braced frames the ability to absorb and dissipate earthquake energy controls the design. Eccentrically braced frames (EBF) are in fact a perfect combination of moment frames and concentrically braced frames, which have sufficient stiffness and ductility properties simultaneously. The stiffness of these systems comes from restraining the lateral displacement by bracing and the ductility of these systems are resulted from using link beams that act as fuses under earthquake loads. A fuse shuts down the current in an electrical circuit when the current becomes more than the capacity of the circuit; therefore, not allowing serious damage to the circuit. This is how a link beam works in EBF systems except that the current in the electrical circuit is in fact the load demand in the building.

Eccentrically braced frames (EBF) were first introduced by Fujimot et al. in 1972 and Tanabashi et al in 1974 [1] in Japan. The major development of this system was due to the ongoing research of Popov and his colleagues from 1977 to 1989 [2] on isolated link beams and other specifications and design criteria of these frames at Berkeley Earthquake Research Center.

In 2005 Richards and Uang [3] studied the rotational capacity of eccentrically braced links by modeling 112 specimens with various widths to thickness ratios of flange. Okazaki et al. (2005) [4] tested various sections and lengths for linked beam under different load protocols to investigate the flange slenderness limit as well as the over strength factor of links.

Berman and Bruneau in 2007 [5], investigated the behavior of tabular links with various thickness, yield strength, and stiffener spacing in eccentrically braced frames experimentally and analytically. They also proposed an equation to prevent buckling of web and flange in tabular link. Berman and Bruneau in 2008 [6] conducted a parametric study on the effect of different geometry and properties of tabular links (web and flange compactness ratios, length of links and stiffener spacing). They also reviewed and developed the design

Haji, M., Azarhomayun, F., Ghiami Azad, A.R. Numerical investigation of truss-shaped braces in eccentrically braced steel frames. Magazine of Civil Engineering. 2021. 102(2). Article No. 10208. DOI: 10.34910/MCE.102.8



This work is licensed under a CC BY-NC 4.0

recommendations for built-up box links located in eccentrically braced frames [7]. In another study by Berman et al. in 2010 [8], the reduced section was applied in links to improve link to column connection ductility. They proposed a design procedure for links with reduced section, and also investigated different geometry and lengths of the reduced section and concluded that the reduced section could reduce the strain of the flange.

Pan et al. in 2011 [9] proposed a new eccentrically braced frame by adding a plate between columns and shear links and investigated its behavior experimentally and numerically. In 2011, Daie et al. [10] used pre-bent strips in a brace as a damper and modeled this device in steel frames with different stories using finite element software in order to investigate its behavior. The results indicated that this system had acceptable stiffness, energy dissipation and deformation capacity. Ohsaki and Nakajima in 2012 [11] optimized the location and thickness of the link member which is used between the beam and eccentrically braced frame by using a heuristic method. They also used the finite element method to obtain the deformation of the link member.

In 2013, Zahrai et al. [12] used a pushover and time-history analysis to evaluate the behavior of an upgraded eccentrically braced frames by adding zipper-struts to the middle of braced span. They concluded that zipper-struts increased the ductility coefficient, displacement, and dissipation capacity. Moreover, this system caused distribution of shear force between shear links by connecting them in all stories and dilation of shear link collapse by increasing the rotational capacity. Irandegani and Narmashiri (2013) [13] used aluminum panels instead of steel in steel braced frame as a vertical link. They modeled the frame in ABAQUS and then modeled 1-, 4-, 8-, and 12-story buildings with different types and shapes of aluminum panels. The aluminum panels increased the energy dissipation. Zahrai and Vosooq in 2013 [14], proposed a new dual system including knee elements at the bottom of the eccentric brace and a new vertical link beams above the eccentric braces. They assessed the behavior of this system and two other systems under monotonic and cyclic loading. The new dual system indicated significant energy dissipation and stable behavior.

Lai and Mahin (2014) [15] examined the seismic behavior of a new strong back system. They concluded that this economic system could decrease the concentration of deformation and damage. Andalib et al. [16] in 2014 studied the effect of different steel rings on ductility and performance of off-center braced frames experimentally and numerically. In 2016, Ashikov et al. [17] investigated a new bolted replaceable active link in the eccentrically braced frame numerically under cyclic loading. They founded that this system increased the rotation capacity and had stable cyclic behavior. Simpson and Mahin in 2017 [18] evaluated a new retrofitting system (strong back) to improve weak story behavior in braced frames. They tested two-story braced frames with two different braces (buckling restrained braces and hollow structural steel braces) in the first story and one hollow structural steel brace in the second story. Their proposed system successfully mitigated the behavior of the weak story. Kafi and Kachooee [19] proposed a new brace with an unbuckled fuse in the middle of brace length and studied its cyclic behavior numerically.

In 2019, Bishay-Girges [20] proposed a new damping system instead of eccentrically braced frames and investigated the effect of this system on the behavior of structures. Naghavi [21] used cables for bracing instead of channels in a steel frame and compared the performance of a cabled frame with a moment frame using the finite element method. The cabled frame considerably increased initial stiffness and load capacity. Mohammadi et al. [22] proposed a new composite buckling restrained fuse and investigated the cyclic behavior of this fuse experimentally and numerically and concluded that this fuse had acceptable ductility and energy absorption. Peng et al. [23] applied finite element modeling to investigate the seismic behavior of eccentric, concentric, and concentric with ring damper braced frames. They concluded that adding ring dampers to concentric braced frame improved the seismic performance such as energy dissipation and load-bearing capacity. Kafi and Nik-Hoosh [24] investigated the geometry of blades in dampers on the behavior of concentric steel frames under static cyclic loading and proposed an optimal length to width ratio for blades.

The main purpose of this study is to investigate the seismic behavior of truss-shaped braces in eccentrically steel braced frames and compare its behavior with conventional braces, which has not been studied so far. Fig. 1 schematically shows the objective of this study. The reason for using truss-shaped braces is that due to the multiplicity and variety of load-bearing elements, the performance (stiffness, stress, pinching, and especially shear strength and energy absorption) of steel frames with such braces can be improved in comparison with conventional braces. Due to the fact that the seismic behavior of this type of braces has not been studied, so in this study, various cross-sections are applied to a new truss-shaped brace and the cyclic behavior of this new brace was investigated and compared to a solid brace. Different parameters, including shear resistance, absorbed energy, stiffness degradation, stress demands, mode of failure and pinching, are obtained and presented for all specimens. In addition, a statistical study is performed to predict absorbed energy, shear capacity and pinching of truss-shaped braces applied in eccentrically steel braced frames with square and circular cross-sections and a reasonably accurate equation is proposed for each case.

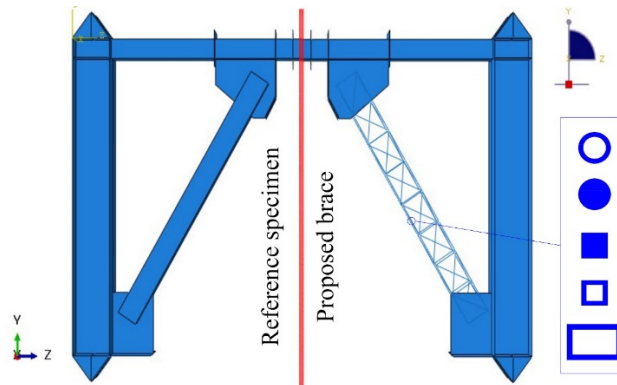


Figure 1. Comparison of the proposed brace comprised of various cross-sections for members with conventional brace.

2. Methods

The use of finite element methods in civil engineering, and especially in the study of concrete and steel structures, has expanded due to its acceptable accuracy and low cost compared to laboratory studies [25]. In this study, the finite element method was used to evaluate the behavior of truss-shaped braces in eccentrically braced steel frames under cyclic loading. First, for the purpose of validation, an experimental frame with an eccentric brace was modeled in ABAQUS software and its results were compared to the experimental specimen. Then the specimens with various brace cross-sections were modeled in ABAQUS and their behavior were studied.

2.1. Model verification

Different eccentric braced frames are presented in Fig. 2 a, b, and c. In this figure, “e” is the length of the link beam. Many experimental studies have been performed on the behavior of eccentric braced steel frames [26–28]. For model verification in finite element software (ABAQUS) [29], a study which was conducted in 2007 by Berman and Bruneau [5], is considered. In the considered frame, the height of the columns is 2460 mm, the length of the beam is 3340 mm, and the length of the braces is 2207 mm. The cross-section of the beam, the column, and the brace are 152×152 mm box, 325×310 wide flange, and 178×178 mm box, respectively. The thickness of the plates used for the flange and the web of columns are 23 and 14 mm, respectively. In addition, the thickness is considered 16 mm, 8 mm, and 11.8 mm for the flange of the beam, the web of the beam, and the braces, respectively. The frame, dimensions and cross-section of the members are shown in Fig. 2d. The thickness of the gusset plates is 13 mm. The modeled gusset plate and its dimensions are shown in Fig. 3.

The frame supports are pinned. In this frame, due to the use of box-shaped cross-sections, the stiffeners are mounted outside the beam to prevent local buckling (Fig. 2d). In order to apply a cyclic lateral load to all specimens, the displacement control method of ASTM E2126-07a [30] was used.

In the study conducted by Berman and Bruneau [5], a hollow rectangular cross-section was applied as link beam in an eccentrically braced frame and the behavior of the frame was investigated. For the purpose of verification, the exact characteristics of the experimental specimen, such as dimensions and cross-sections of the frame and the brace, mechanical properties of steel and the beam to column connection properties were derived from the experimental specimen and were modeled in the finite element software.

The static general analysis in Abaqus was used in this study. The type of elements which were used for meshing the frame, and the proposed brace were shell (S4R), and beam (B31), respectively. The approximate global size of 10 was employed for the mesh size, which was selected based on the accuracy of the results of the verification study. Based on the study by Bruneau and Berman [5], two types of grade 50 steel (elastic-perfectly plastic model) were used for the flange and the web (Fig. 4). The yield stress of steel for the web and the flange material was defined 448 and 393 MPa, respectively. The values of density, young's modulus and Poisson's ratio were taken to be 785 kg/m³, 210000 MPa and 0.3 respectively for both types of steels. The displacement of the frame was measured at a point above the column (U3). Also, the support reaction force (RF3) was obtained in the z-direction for the displacements applied to the specimen. In order to plot the cyclic curve, these values were plotted together.

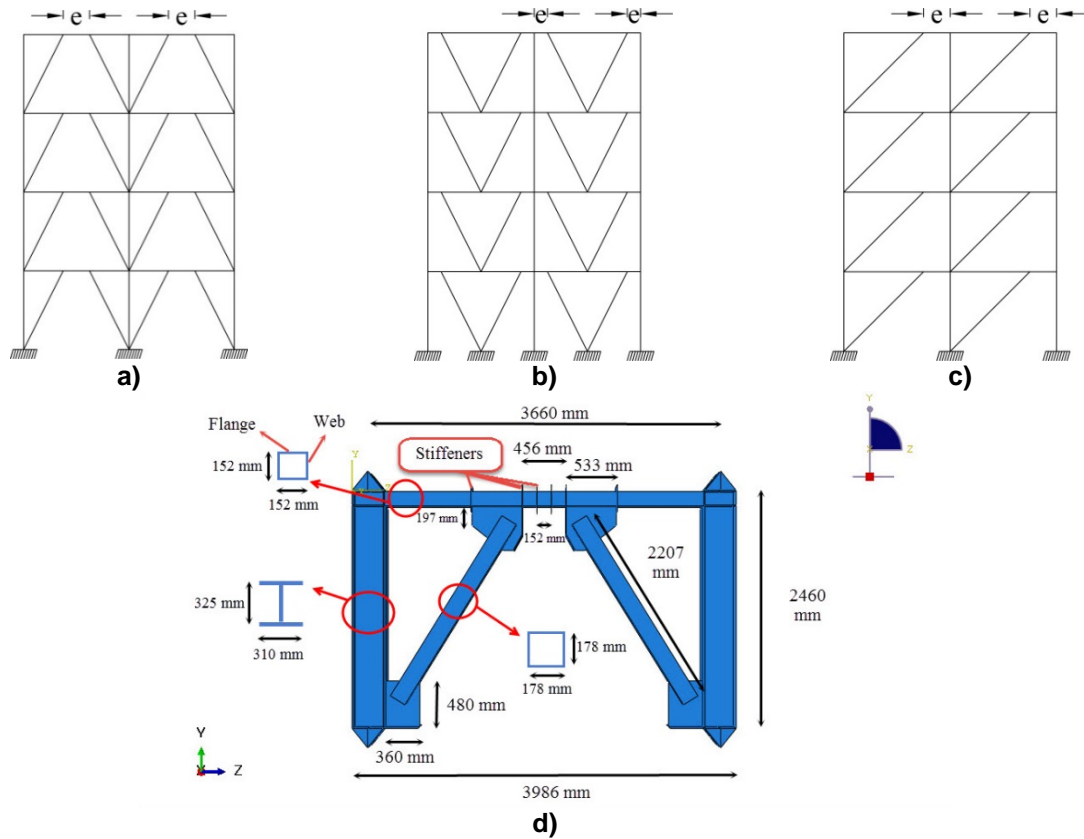


Figure 2. a, b, c) Different types of eccentric braced frames, and d) Dimensions of modeled frame for verification.

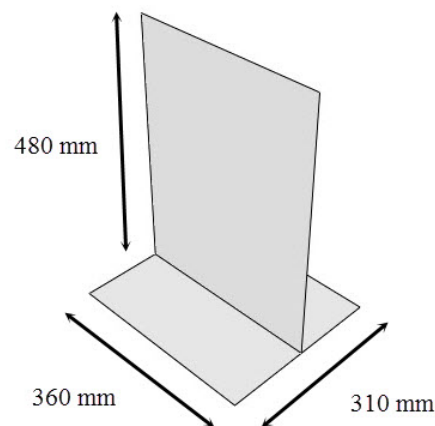


Figure 3. Dimensions of the gusset plate.

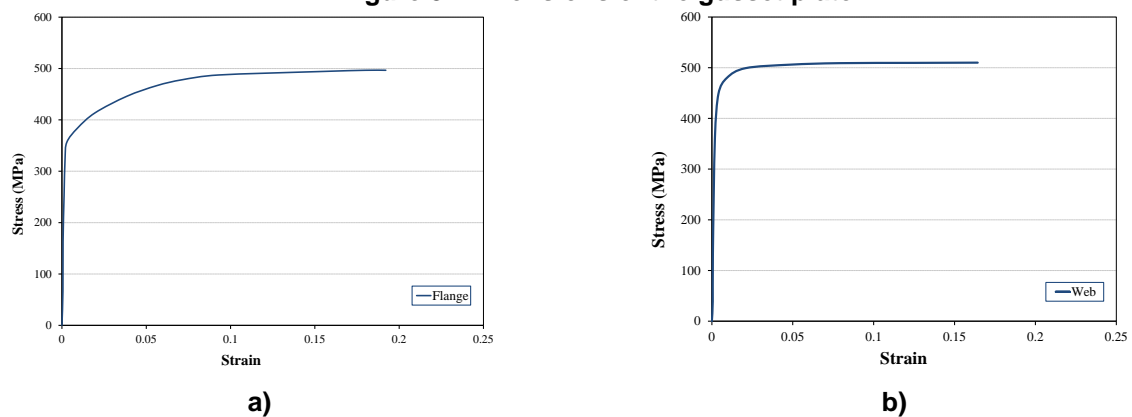


Figure 4. Stress-strain diagrams of steels which were used for a) Flange (type 1), and b) web (type 2) in the experimental study [5].

The ATC-24 [31] loading protocol is used which was used in the Berman and Bruneau study [5]. The rotation of the link beam versus its shear was obtained and was compared to the experimental results. In Fig. 5 the comparison of these two graphs are presented. As shown in this figure, the numerical modeling exhibits reasonable correlation with the experimental results. Although certain correlation between the graphs is observed, some difference is also clearly seen. Differences in experimental and numerical results can be due to two general items: 1. Experimental errors: errors caused by laboratory equipment such as lack of instrumentation calibration, human errors during testing, etc. 2. Errors of numerical methods: these errors can be due to modeling errors, use of simplification hypotheses and techniques (in defining materials, type of connections and supports, and etc.), type of elements, type of analysis, number of degrees of freedom, and etc. Because of all the aforementioned inevitable uncertainties, the difference observed in this study can be acceptable.

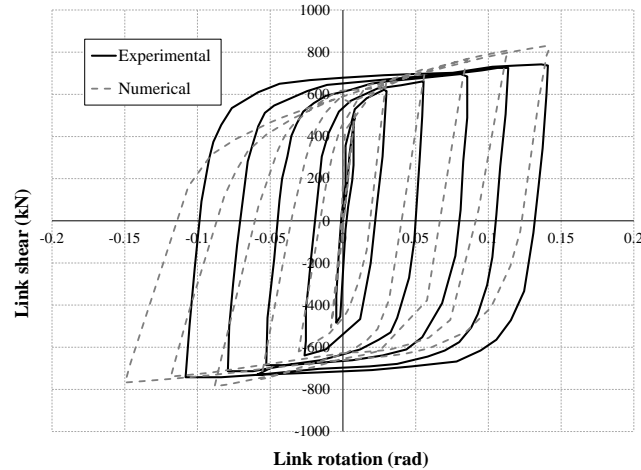



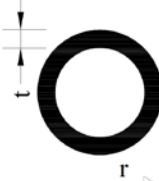
Figure 5. Comparison of experimental results with numerical results.

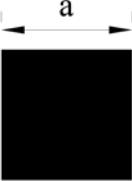

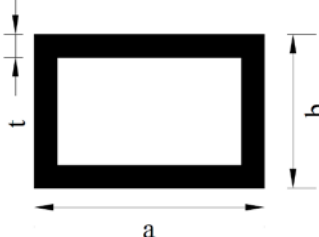
2.2. Proposed models

In this study, a reference specimen similar to the specimen intended for validation, and 10 specimens similar to the reference specimen but braced with truss-shaped brace (which is shown in Fig. 6) were modeled. Various cross-sections (Table 1) were considered for all the members of truss-shaped brace to investigate the behavior of these braces located in the eccentrically braced steel frame instead of the ordinary brace with a solid section. Six groups of sections including solid and hollow circle, square and rectangle with different dimensions were considered. The mechanical properties of steel (Fig. 4) in all specimens were considered the same as the verified model. For all members, type 1 steel was used except for the web of the beam and column, in which type 2 steel was used.

The geometry of each cross-section, its dimensions, specimen's name, and the moment of inertia of each cross-section are provided in Table 1. Due to the availability of sections in the market, the dimensions of the sections were selected from the Stahl table [32].

Table 1. Cross-sections used in the braces.

Cross-section	Dimensions (cm)	Specimen Name	Moment of Inertia (cm^4)
	$r = 1.75$	CS1	7.36
	$r = 2$	CS2	12.56
	$r = 3.8, t = 0.4$	CH1	58.78
	$r = 4.45, t = 0.6$	CH2	135.36

Cross-section	Dimensions (cm)	Specimen Name	Moment of Inertia (cm^4)
	$a = 3.2$	SS1	8.74
	$a = 3.5$	SS2	12.5
	$a = 6, t = 0.5$	SH1	31.75
	$a = 10, t = 0.4$	SH2	125.54
	$a = 9, b = 5, t = 0.4$	RH1	59.93
	$a = 12, b = 8, t = 0.4$	RH2	163.43

Due to the size of the cross-sections (one relatively smaller dimension compared to other dimensions), all the elements were modeled by shell elements, except for the braces in the reference specimen, which was modeled with beam elements. The Standard reduced integration shell element type (S4R) was selected for mesh element type, which reduced the computation time without significant effect on the results. Furthermore, a beam element was used to mesh the braces. All the members of frame were merged, and tie constraints were used to connect the braces to the frame. In order to take into account the buckling effect in members, the imperfection load was applied to the frame. In Fig. 6 the geometry of the proposed brace and its dimensions are shown. The sections in Table 1 are used for the members of the proposed brace.

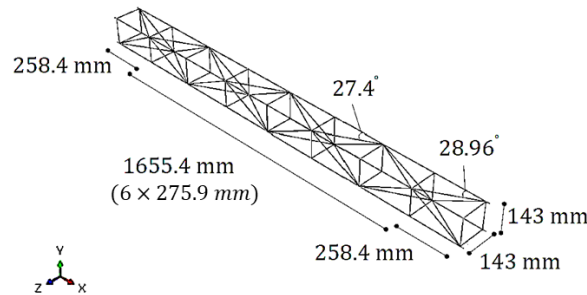


Figure 6. The proposed brace implemented in the steel frame.

3. Results and Discussion

In this section, the results of finite element modeling, such as hysteresis curve, absorbed energy, stiffness degradation, stress, mode of failure and pinching, are presented for all the specimens. The results are compared with each other, as well as with the reference specimen, which is the verified model of the specimen experimentally investigated by Bruneau and Berman [5].

3.1. Hysteresis Curves

To assess the seismic behavior of the proposed braces, a cyclic displacement was applied to the top of the columns. The protocol applied to the specimen includes displacements of 12, 15, 21, 30, 45, 60, 85, 105, 135, 150, 195 mm. In order to consider the buckling effect, an eccentric load was applied to the left side of the link beam. As shown in Fig. 7a, this force generates a very small displacement at the left side of the beam. The hysteresis curves of all specimens are presented in Fig. 8. The displacement value was measured at a point above the column (Fig. 7b).

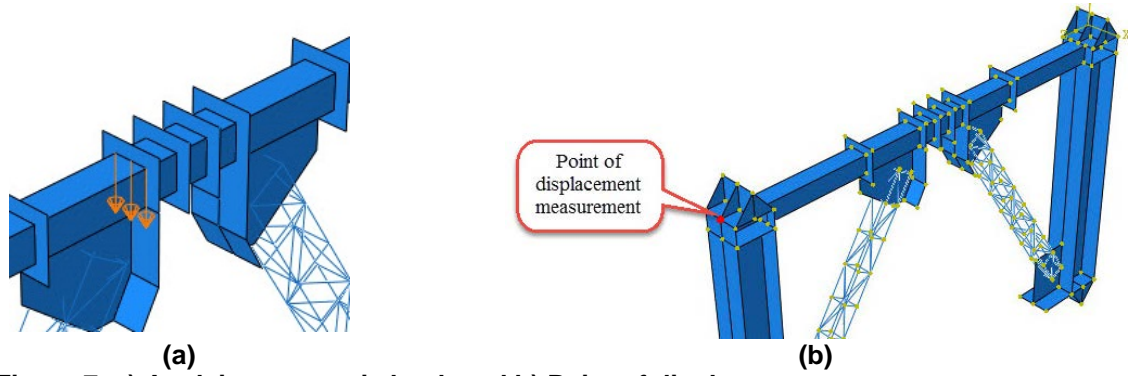
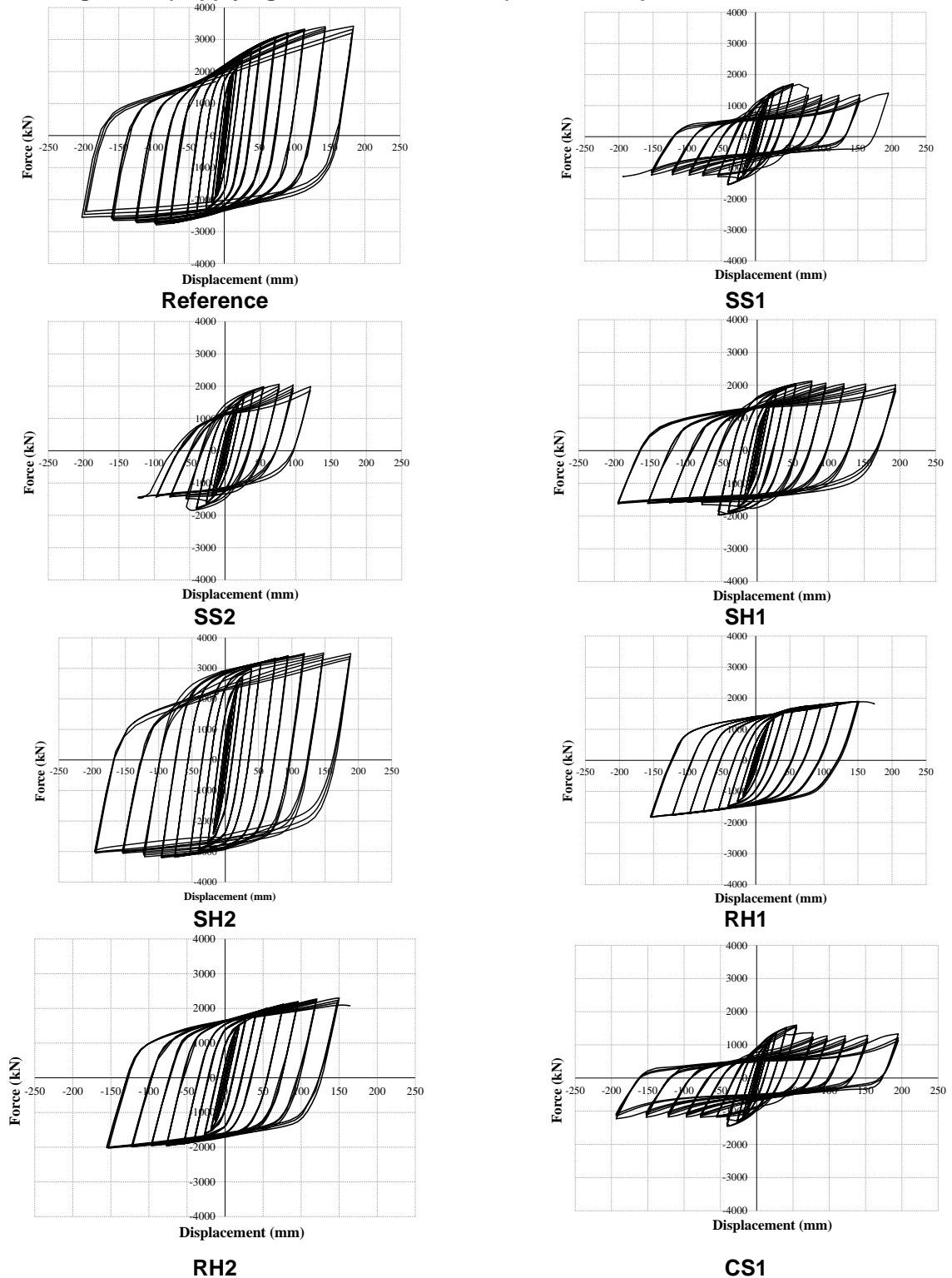


Figure 7. a) Applying eccentric load, and b) Point of displacement measurement.



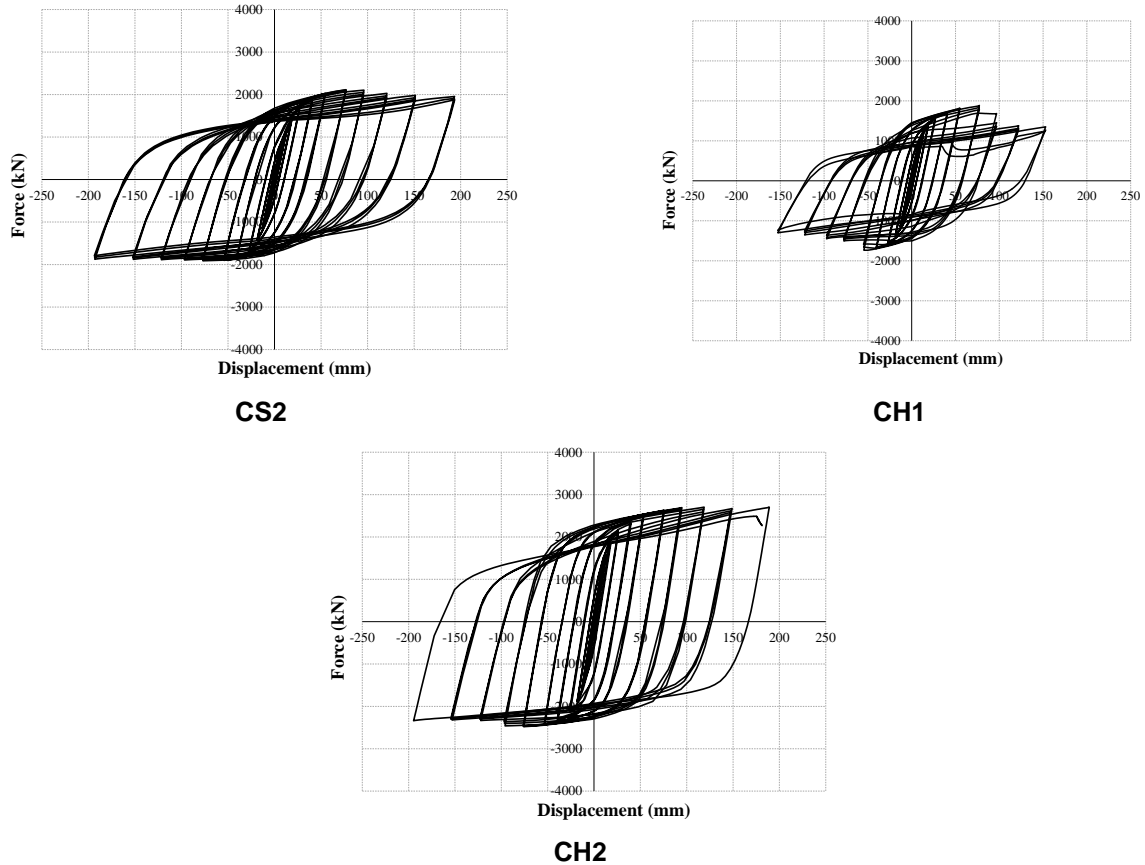


Figure 8. Hysteresis curves of specimens.

3.2. Absorbed Energy

The meaning of absorbed energy in this section is the area under the force-displacement cyclic curve. In order to compare the absorbed energies in all specimens, this parameter was computed up to the displacement of 150 mm and is present in Table 2. The maximum shear strength tolerated by each specimen is also presented in Table 2. In addition, the difference of absorbed energy and shear strength in all specimens compared to the reference specimen was computed and presented in percent.

Table 2. Comparison of the absorbed energy, and shear strength values of the proposed specimens with those of the reference specimen.

Specimen name	Absorbed Energy (kN.mm)	Difference with the Reference Specimen (%)	Shear Strength (kN)	Difference with Reference Specimen (%)
Reference	1.06E+07	---	3420.11	---
SS1	3.85E+06	63.57	1705.65	50.13
SS2	3.95E+06	62.67	2062.81	39.68
SH1	7.26E+06	31.35	2130.79	37.7
SH2	1.1E+07	-30.71	3510.46	-2.64
RH1	6.71E+06	36.54	1896.92	44.54
RH2	8.35E+06	21.07	2302.31	32.68
CS1	3.60E+06	65.93	1598.85	53.25
CS2	7.52E+06	28.93	2113.55	38.2
CH1	5.24E+06	50.48	1884.48	44.9
CH2	1.05E+07	1.15	2705.13	20.9

In this table the negative sign indicates an increase in the desired parameter compared to the reference specimen. As shown in Table 2, all the specimens showed lower absorbed energy and shear capacity compared to the reference specimen except specimen SH2 with 30.71 % and 2.64 % increase in absorbed energy and shear capacity, respectively. Moreover, in specimen CH2 the results are almost similar to the reference specimen.

In each cross-section with defined geometry, absorbed energy and shear strength increased with increasing cross-section dimensions. The hollow sections indicated acceptable results compared to solid sections such that the hollow square, circle, and rectangular geometries had the top three best responses, respectively. In solid cross-sections, the square cross-section also showed better performance than the circle geometry.

3.3. Stiffness Degradation

The diagram of secant stiffness versus displacement for all the specimens in the positive direction (the direction with the greatest force tolerated) is shown in Fig. 9. To obtain the secant stiffness, the maximum force in three cycles with equal displacement (first cycle) was divided by its corresponding displacement. As indicated in Fig. 9, the reference specimen (indicated by "R" in the figure), SH2, CH2 and CS1 specimens exhibited the highest initial stiffness, respectively. As the displacement increased from 19 mm to 125 mm, specimen SH2 followed by the reference specimen showed the highest stiffness. Moreover, stiffness degraded faster in specimens SS1, CS1 and RH1.

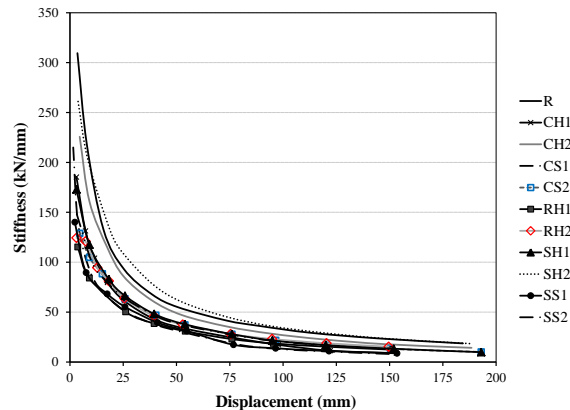
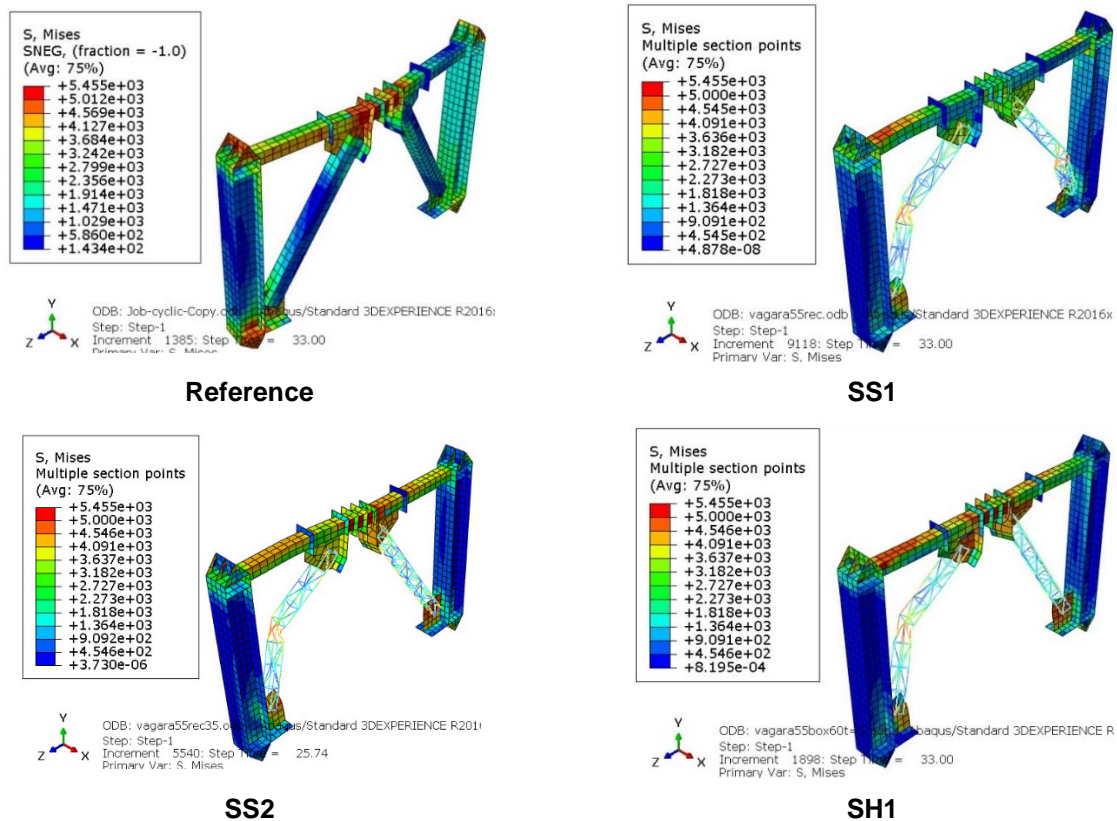


Figure 9. Stiffness degradation versus displacement for all specimens.

3.4. Von Mises Stresses and Modes of Failure

The von Mises stress values in braced frames are presented at the end of loading for all specimens in Fig. 10. The modes of failure can be seen in this figure as well.



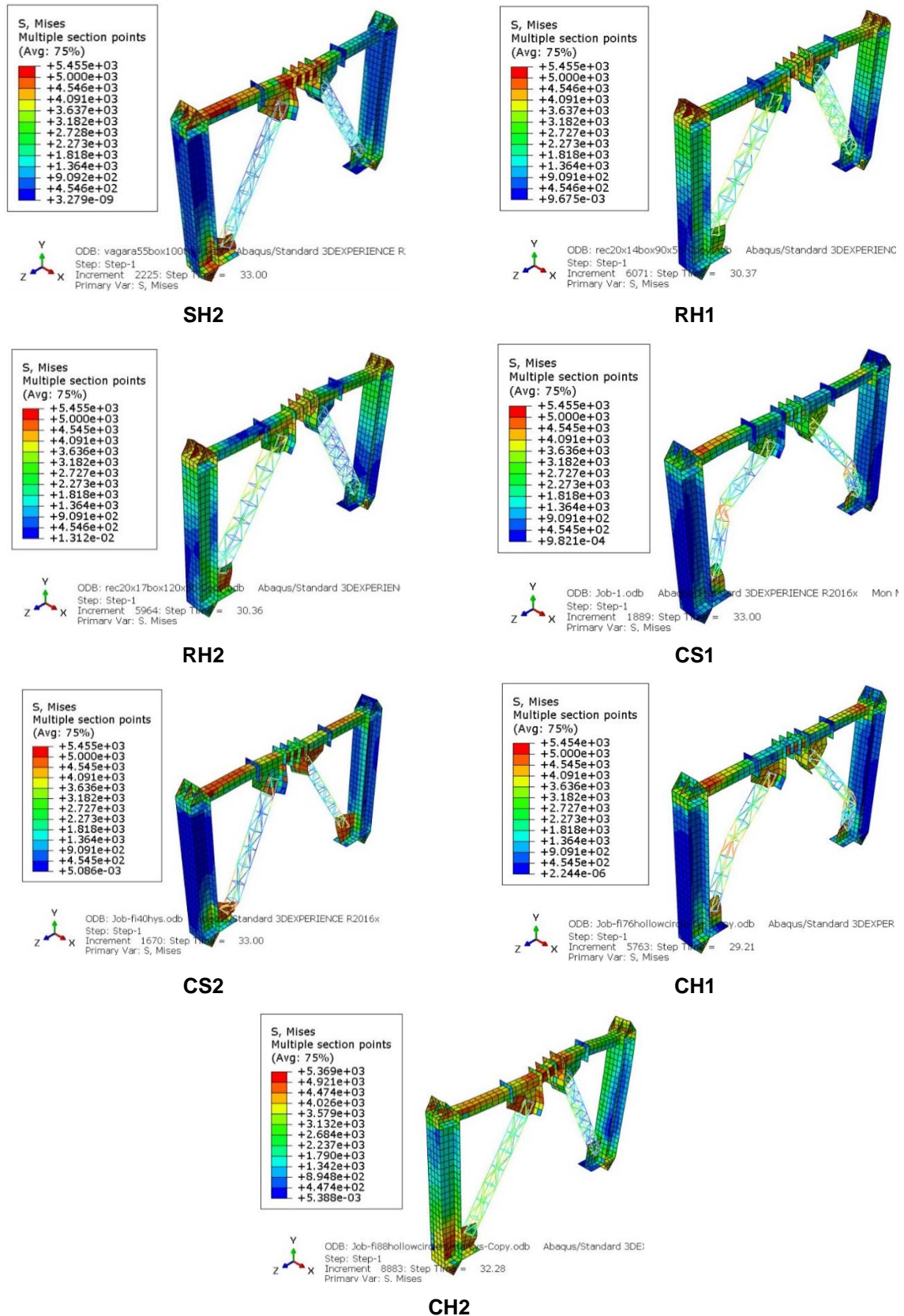


Figure 10. The stresses (kg/cm²) in all specimens at the end of loading.

As seen in Fig. 10, the maximum stresses in the reference specimen, SS2, SH1, SH2, CS2 and CH2 happened in the linked beam. The stress distribution in specimen SH2 is remarkably close to that of the reference specimen, while specimen RH1 had the lowest stress in the beam compared to other specimens. In specimens SS1, RH1, RH2, and CH2, the stresses in the beam are lower and more stress is tolerated by the braces and gusset plates compared to other specimens. The connections between the beams and columns are fixed to withstand the moment caused by lateral loads (earthquake or wind) in addition to vertical shear stress. If the beam-to-column connection is fixed, the moment tolerated by the beam and the column is greater

that tolerated by the brace. In terms of shear, shear tolerated by the column and the brace is greater than that tolerated by the fixed joint.

The brace buckling occurred in specimens SS1, SS2, SH1, CS1 and CH1 while in other specimens such as SH2, RH1, RH2, CS2, and CH2 the left gusset plate distortion was observed, which is shown in Fig. 11. In cyclic loading, the first force that caused out of plane movement of the braces was considered as the buckling force. The buckling force of these specimens are presented in Table 3. In this table, the buckling load is the load that causes the brace to buckle. The negative sign means that buckling occurred first in the left brace. According to Table 3 the specimens with solid circle (CS1) and hollow square cross-sections (SH1) had the lowest and highest buckling load, respectively, whereas the braces with rectangular cross-sections did not experience buckling in the brace.

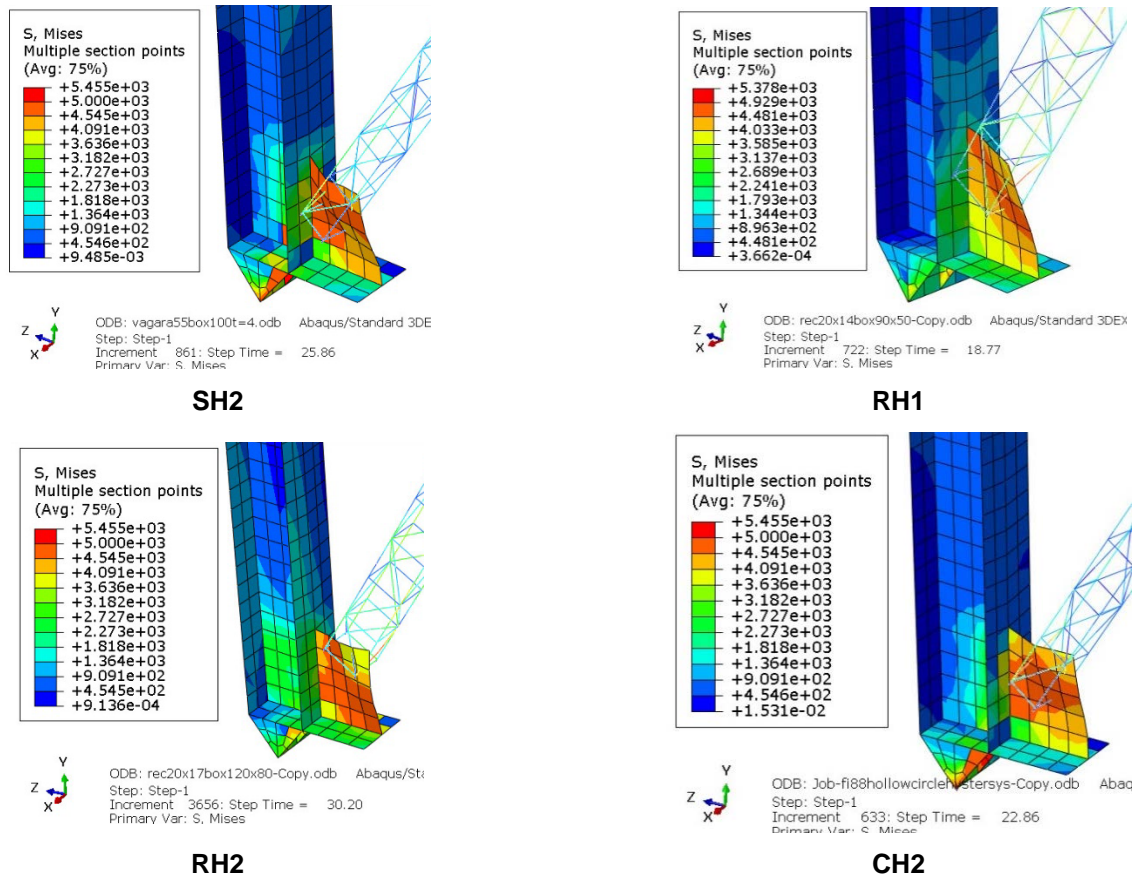


Figure 11. The gusset plate distortion.

Table 3. Buckling loads of specimens.

Specimen	Buckling Load (kN)
SH2	-1544.98
SS2	-1839.41
SH1	-1853.15
CS1	-1116.06
CH1	-1733.94

In the reference specimen, the beam was deflected and moved out of plane (Fig. 12), whereas this deflection was not seen in specimens SH2 and CH2. This may be attributed to the fact that the beam is weaker than the braces in the reference specimen. Therefore, before the braces can withstand much stress, the beam undergoes non-linear and plastic deformation and moves out of its plane.

According to Table 3 the specimens with solid circle (CS1) and hollow square cross-sections (SH1) had the lowest and highest buckling load, respectively, whereas the braces with rectangular cross-sections did not experience buckling in brace.

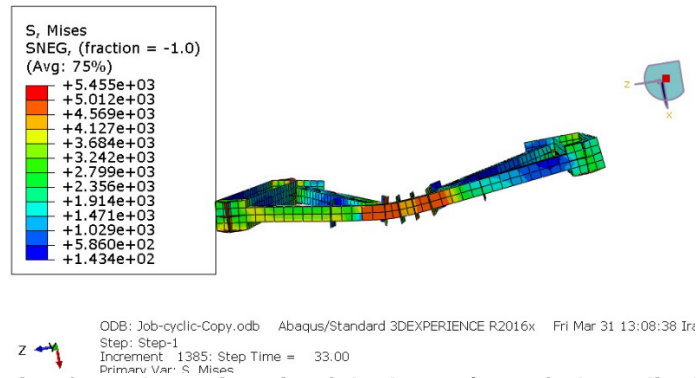


Figure 12. Deviation from the main axis of the beam (out-of-plane displacement) in the reference specimen.

3.5. Pinching

Pinching is the amplitude of the force which corresponds to the maximum force range tolerated by the specimen. The distance between the minimum and maximum force tolerated by the specimen on the vertical part of the cyclic diagram is defined as pinching. Pinching is a measure of the degree of ductility and energy absorption of a specimen. The smaller the amount of pinching is, the more flexible and ductile the behavior of the frame is [33]. Pinching is defined by parameter "X" in Fig. 13. Pinching was calculated for all specimens and is presented in Table 4. To calculate pinching, the distance between maximum and minimum forces in vertical axis was determined and presented. Note that more pinching means that the distance "X" in Fig. 13 is in fact smaller.

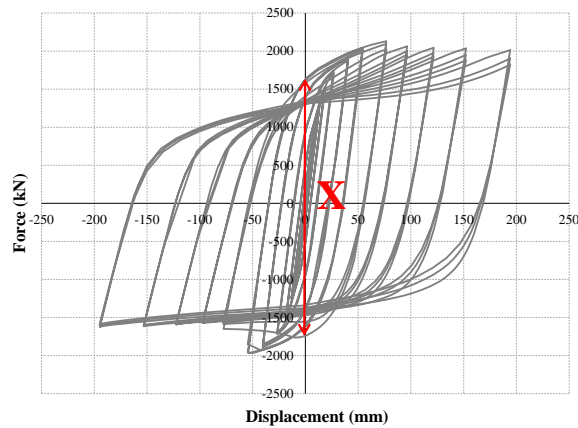


Figure 13. Pinching in hysteresis curve.

Table 4. The amount of pinching for all specimens.

Specimen name	Pinching (kN)
Reference	4579.71
SS1	2235.3
SS2	2930.67
SH1	3407.17
SH2	5915.96
RH1	2867.65
RH2	3382.35
CS1	1949.787
CS2	3413.87
CH1	2966.39
CH2	4588.23

According to Table 4, the amount of parameter "X" in SH2, CH2 and the reference specimen is more than that in other specimens. This means that specimens SH2, CH2 have ductile and flexible behavior.

3.6. Prediction

In this section, prediction means obtaining the values of absorbed energy, shear strength and pinching for frames with truss-shaped braces based on the results obtained in this study. According to the results, as

well as the moments of inertia for each section, the prediction of each result was performed using trend lines. Diagram of absorbed energy, shear strength and pinching changes versus moment of inertia for each section in each group (circle and square) was plotted and the best relationship was obtained for each case using trend lines. These diagrams for the circular and square sections are shown in Fig. 14 and 15, respectively. In these figures, the points are the values obtained by the finite element method and the lines are regression lines. In each diagram, the values of R^2 for the regression lines are provided, which indicates the accuracy of the prediction. In each case, the best type of regression which had a value of R^2 closer to one was selected.

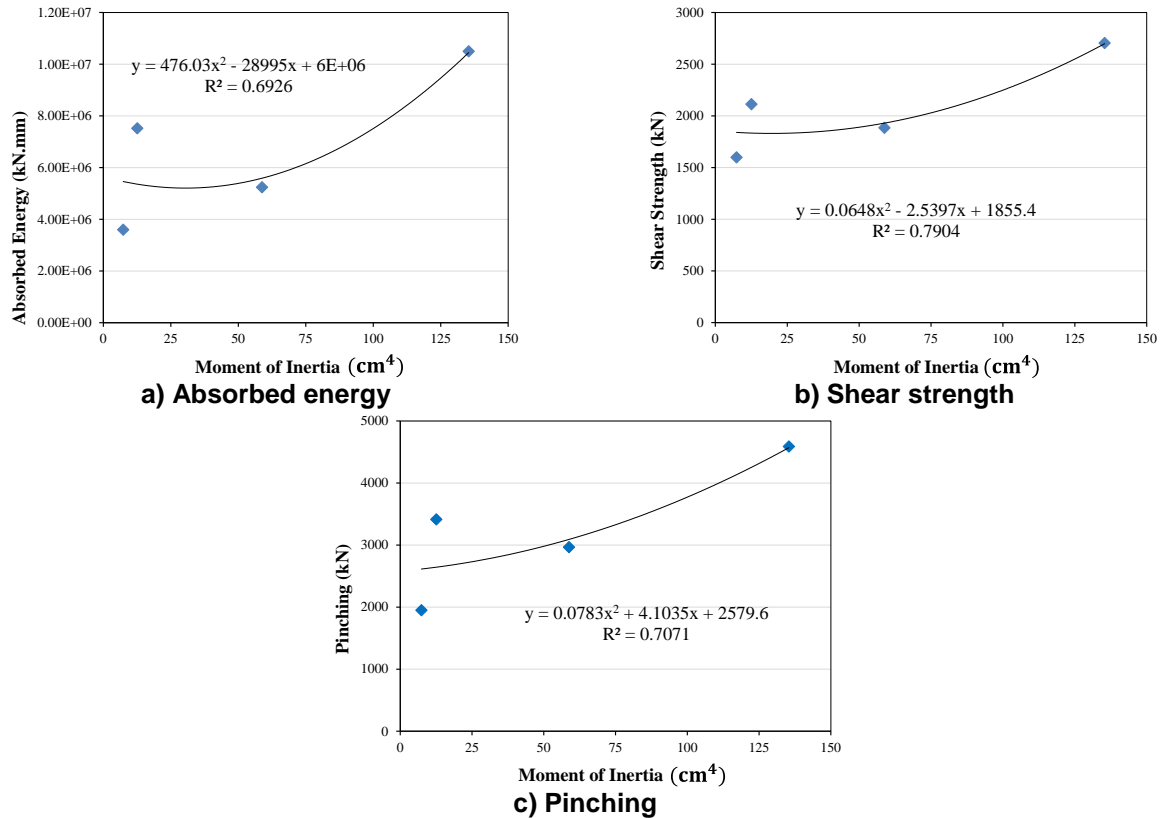


Figure 14. Regression of results for circular cross-sections.

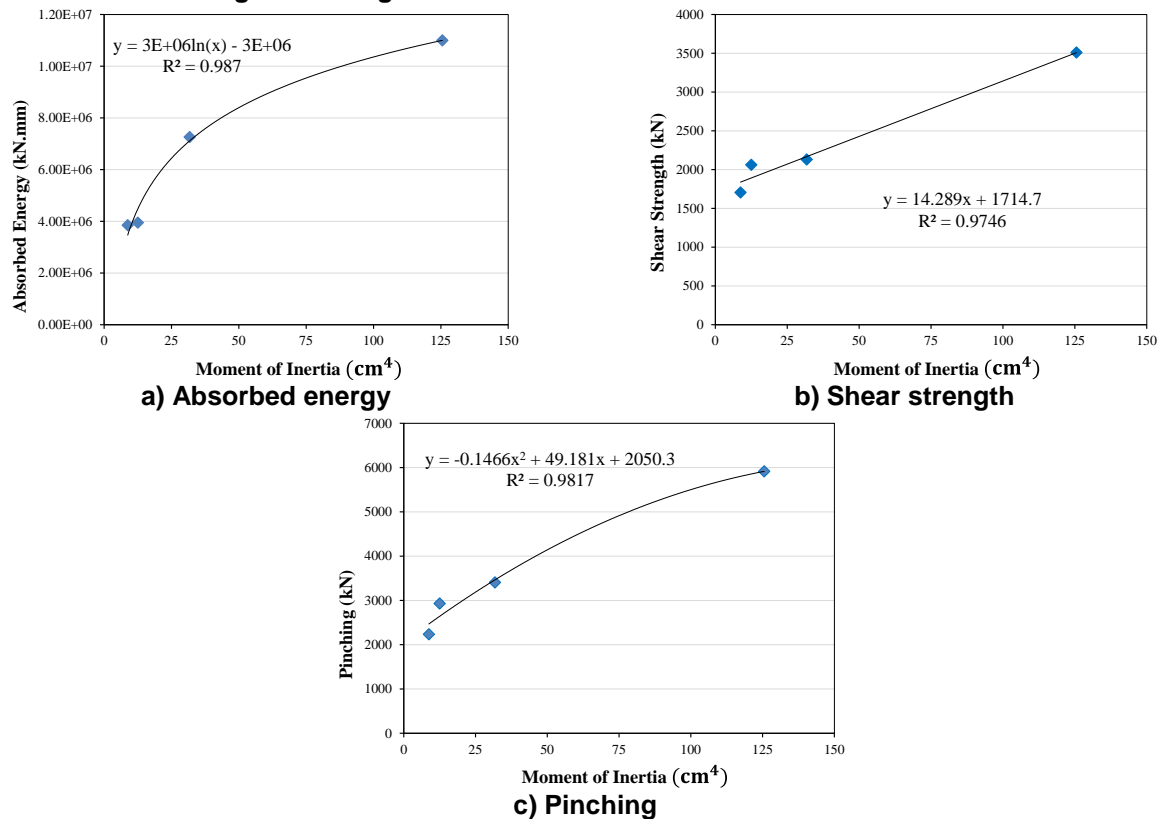


Figure 15. Regression of results for square cross-sections.

For both circular and square sections, second order polynomial was used as regression type to predict the results. However, a logarithmic function was considered for regression in square sections for absorbed energy. The values of R^2 for the square sections are closer to one than the circular sections, indicating better performance of the considered functions in predicting the results for these sections.

4. Conclusion

In this paper, a new truss-shaped brace was proposed, and the cyclic behavior of this new brace was investigated numerically. The variables in the models included the geometric shapes of the cross-section (solid/hollow and circle/square/rectangular). Nonlinear analysis was performed by finite element software, the results were obtained and some parameters such as shear strength, absorbed energy, stiffness degradation, stress, failure mode and pinching were presented for all specimens and compared to the reference specimen. Also, some equations were presented based on obtained results for the absorbed energy, shear strength, and pinching of circular and square cross-sections versus moment of inertia. The most important results are as follow:

- In terms of absorbed energy, the hollow square section with width and thickness of 100 and 4 mm (SH2), with 30.71 % increase compared to the reference specimen showed the best performance among all specimens. In the brace with hollow circular cross-section with the radius of 44.5 mm and the thickness of 6 mm, the absorbed energy was almost similar to the reference specimen. Also, the same results were obtained for the shear strength, except that the amount of increase in shear strength compared to the reference specimen was 2.64 % in SH2.
- The brace buckling was observed in at least one of each cross-section shapes, except in the braces with hollow rectangular cross-section. The lowest stresses in the frame due to cyclic loading were also observed in the braces with this kind of cross-section. Among the buckled braces, the braces with solid circular cross-section and hollow square cross-section had the lowest and highest buckling load, respectively.
- Initial stiffness in the reference specimen and SH2 specimens had the highest amounts and the stiffness reduction rate in these two specimens was minimal in comparison with other specimens.
- It can be concluded from the pinching values that the new brace with hollow square cross-section with bigger dimensions (SH2) with 29.18 % increase in pinching compared to the reference specimen showed more ductile behavior than the rest of the specimens.

Finally, by increasing the moment of inertia of the proposed brace cross-section, its performance such as shear capacity, absorbed energy, stiffness degradation, stresses in members, mode of failure and pinching, improves. However, more research is required to better understand the behavior of truss-shaped braces in eccentrically braced frames. Conducting full-scale experiments are highly recommended to further back up the results of this study. In addition, studying this brace in concentrically braced frames is recommended to better understand the behavior of this type of brace.

References

1. Tanabashi, R., Naneta, K., Ishida, T. On the rigidity and ductility of steel bracing assemblage. Proceedings of the 5th World Conference on Earthquake Engineering. Rome, 1974. Pp. 834–840.
2. Popov, E.P., Kasai, K., Engelhardt, M.D. Advances in design of eccentrically braced frames. Earthquake Spectra. 1987. 3(1). Pp. 43–55.
3. Richards, P.W., Uang, C.M. Effect of flange width-thickness ratio on eccentrically braced frames link cyclic rotation capacity. Journal of Structural Engineering. 2005. 131(10). Pp. 1546–1552. DOI: 10.1061/(ASCE)0733-9445(2005)131:10(1546)
4. Okazaki, T., Arce, G., Ryu, H.C., Engelhardt, M.D. Experimental study of local buckling, overstrength, and fracture of links in eccentrically braced frames. Journal of Structural Engineering. 2005. 131(10). Pp. 1526–1535. DOI: 10.1061/(ASCE)0733-9445(2005)131:10(1526)
5. Berman, J.W., Bruneau, M. Experimental and analytical investigation of tubular links for eccentrically braced frames. Engineering Structures. 2007. 29(8). Pp. 1929–1938. DOI: 10.1016/j.engstruct.2006.10.012
6. Berman, J.W., Bruneau, M. Tubular links for eccentrically braced frames. I: Finite element parametric study. Journal of Structural Engineering. 2008. 134(5). Pp. 692–701. DOI: 10.1061/(ASCE)0733-9445(2008)134:5(692)
7. Berman, J.W., Bruneau, M. Overview of the development of design recommendations for eccentrically braced frame links with built-up box sections. Engineering Journal-American Institute of Steel Construction. 2013. 50(1). Pp. 21–31.
8. Berman, J.W., Okazaki, T., Hauksdottir, H.O. Reduced link sections for improving the ductility of eccentrically braced frame link-to-column connections. Journal of Structural Engineering. 2010. 136(5). Pp. 543–553. DOI: 10.1061/(asce)st.1943-541x.0000157
9. Pan, X., Hao, J., Gao, J. Study of adding cover-plate used for the single diagonal eccentrically braced steel frames. Open Civil Engineering Journal. 2011. No. 5. Pp. 143–153.
10. Daie, M., Jalali, A., Suhatri, M., Shariati, M., Arabnejad Khanouki, M.M., Shariati, A., Kazemi-Arbat, P. A new finite element investigation on pre-bent steel strips as damper for vibration control. International Journal of the Physical Sciences. 2011. 6(36). Pp. 8044–8050. DOI: 10.5897/IJPS11.1585
11. Ohsaki, M., Nakajima, T. Optimization of link member of eccentrically braced frames for maximum energy dissipation. Journal of Constructional Steel Research. 2012. No. 75. Pp. 38–44. DOI: 10.1016/j.jcsr.2012.03.008

12. Zahrai, S.M., Pirdavari, M., Momeni Farahani, H. Evaluation of hysteretic behavior of eccentrically braced frames with zipper-strut upgrade. *Journal of Constructional Steel Research*. 2013. No. 83. Pp. 10–20. DOI: 10.1016/j.jcsr.2012.12.017
13. Irandegani, M.A., Narmashiri, K. Numerical study on aluminum panels used in braced steel frames as energy dissipation systems. *International Journal of Physical Sciences*. 2012. 7(10). Pp. 1661–1669.
14. Vosooq, A.K., Zahrai, S.M. Study of an innovative two-stage control system: Chevron knee bracing & shear panel in series connection. *Structural Engineering and Mechanics*. 2013. 47(6). Pp. 881–898. DOI: 10.12989/sem.2013.47.6.881
15. Lai, J.W., Mahin, S.A. Strongback system: a way to reduce damage concentration in steel-braced frames. *Journal of Structural Engineering*. 2015. 141(9). Pp. 04014223. DOI: 10.1061/(ASCE)ST.1943-541X.0001198
16. Andalib, Z., Kafi, M.A., Kheyroddin, A., Bazzaz, M. Experimental investigation of the ductility and performance of steel rings constructed from plates. *Journal of Constructional Steel Research*. 2014. 103. Pp. 77–88. DOI: 10.1016/j.jcsr.2014.07.016
17. Ashikov, A., Clifton, G.C., Belev, B. Finite element analysis of eccentrically braced frames with a new type of bolted replaceable active link. *New Zealand Society for Earthquake Engineering (NZSEE) Annual Technical Conference*. Christchurch, 2016. Pp. 1–9.
18. Simpson, B.G., Mahin, S.A. Experimental and numerical investigation of strongback braced frame system to mitigate weak story behavior. *Journal of Structural Engineering*. 2018. 144(2). Pp. 04017211. DOI: 10.1061/(ASCE)ST.1943-541X.0001960
19. Kafi, M.A., Kachooee, A. The behavior of concentric brace with bounded fuse. *Magazine of Civil Engineering*. 2018. 78(2). Pp. 16–29.
20. Bishay-Girges, N.W. An Alternative system for eccentrically braced frames resisting lateral loads. *Engineering, Technology & Applied Science Research*. 2019. 9(3). Pp. 4281–4286.
21. Naghavi, M.S. Retrofitting steel moment frames using cable bracing. *Journal of Building Material Science*. 2019. 1(01). Pp. 10–17.
22. Mohammadi, M., Kafi, M.A., Kheyroddin, A., Ronagh, H.R. Experimental and numerical investigation of an innovative buckling-restrained fuse under cyclic loading. *Structures*. 2019. 22. Pp. 186–199. DOI: 10.1016/j.istruc.2019.07.014
23. Peng, X., Lin, C., Cao, Y., Duan, W. Nonlinear finite element simulation on seismic behavior of steel frame-central brace with ring damper. *IOP Conference Series: Materials Science and Engineering*. 2019. 472. Pp. 012031. DOI: 10.1088/1757-899X/472/1/012031
24. Kafi, M.A., Nik-Hoosh, K. Geometry of steel slit dampers in a braced steel frame under cyclic loading. *Magazine of Civil Engineering*. 2019. 87(3). Pp. 3–17.
25. Haji, M., Naderpour, H., Kheyroddin, A. Strengthening of reinforced concrete bridge columns with FRP, using wrapping, near-surface mounted and combined methods. *Journal of Transportation Infrastructure Engineering*. 2018. 3(4). Pp. 33–48.
26. Popov, E.P., Engelhardt, M.D. Seismic eccentrically braced frames. *Journal of Constructional Steel Research*. 1988. 10. Pp. 321–354. DOI: 10.1016/0143-974X(88)90034-X
27. Wang, F., Su, M., Hong, M., Guo, Y., Li, S. Cyclic behavior of Y-shaped eccentrically braced frames fabricated with high-strength steel composite. *Journal of Constructional Steel Research*. 2016. 120. Pp. 176–187. DOI: 10.1016/j.jcsr.2016.01.007
28. Mansour, N., Christopoulos, C., Tremblay, R. Experimental validation of replaceable shear links for eccentrically braced steel frames. *Journal of Structural Engineering*. 2011. 137(10). Pp. 1141–1152. DOI: 10.1061/(ASCE)ST.1943-541X.0000350
29. HKS. ABAQUS standard user's manual. Hibbitt, Karlsson, and Sorensen, Inc. 2001.
30. ASTM. Standard test methods for cyclic (reversed) load test for shear resistance of vertical elements of the lateral force resisting systems for buildings. 2009.
31. ASTM. Standard test methods and definitions for mechanical testing of steel products, A370-03a. ASTM International. 2003.
32. EN 10365 – The European Norm for Structural Sections in Steel. 2017.
33. Haji, M., Naderpour, H., Kheyroddin, A. Experimental study on influence of proposed FRP-strengthening techniques on RC circular short columns considering different types of damage index. *Composite Structures*. 2019. 209. Pp. 112–128. DOI: 10.1016/j.compstruct.2018.10.088

Contacts:

Mohammad Haji, mohammadhaji@semnan.ac.ir

Fazel Azarhomayun, fazel.azarhomayun@ut.ac.ir

Amir Reza Ghiami Azad, rghiami@ut.ac.ir

© Haji, M., Azarhomayun, F., Ghiami Azad, A.R., 2021